

## Winter Eddy Genesis in the Eastern South China Sea due to Orographic Wind Jets

GUIHUA WANG

*State Key Laboratory of Satellite Ocean Environment Dynamics, Second Institute of Oceanography, State Oceanic Administration, Hangzhou, China*

DAKE CHEN

*State Key Laboratory of Satellite Ocean Environment Dynamics, Second Institute of Oceanography, State Oceanic Administration, Hangzhou, China, and Lamont-Doherty Earth Observatory, Columbia University, Palisades, New York*

JILAN SU

*State Key Laboratory of Satellite Ocean Environment Dynamics, Second Institute of Oceanography, State Oceanic Administration, Hangzhou, China*

(Manuscript received 22 June 2007, in final form 10 August 2007)

### ABSTRACT

Generation of mesoscale eddies in the eastern South China Sea (SCS) in winters during August 1999 to July 2002 is studied with a reduced-gravity model. It is found that the orographic wind jets associated with the northeast winter monsoon and the gaps in the mountainous island chain along the eastern boundary of the SCS can spin up cyclonic and anticyclonic eddies over the SCS. Results suggest that direct wind forcing could be an important generation mechanism for the rich eddy activity in the SCS, and that to simulate this mechanism the resolution of the wind forcing has to be high enough to resolve the local wind jets induced by orographic effects.

### 1. Introduction

The South China Sea (SCS) is the largest semienclosed marginal sea in the northwest Pacific (Fig. 1). The large-scale circulation in the SCS is driven mainly by the east Asian monsoon, with significant influence from the Kuroshio in its northern part (Qu 2000; Su 2004). In winter there is generally a cyclonic gyre over the deep basin of the SCS, while in summer a cyclonic gyre remains north of about 12°N and an anticyclonic gyre prevails to the south. The basic features and dynamics of this large-scale circulation have been studied with various numerical models using different wind products (e.g., Metzger and Hurlburt 2001; Liu et al. 2001; Metzger 2003).

Embedded in the basin-scale circulation are numerous mesoscale eddies, as evident in both hydrographic data (Chu et al. 1998; Su et al. 1999) and altimeter observations (Shaw et al. 1999; Hwang and Chen 2000; Wang et al. 2003). Based on 5 yr of altimetry from 1992 to 1997, significant mesoscale variability is found in the SCS in two strips north of 10°N (Wang et al. 2000). One lies along the northern/western boundary of the deep basin near the 2000-m isobath over the lower continental slope. The other is a northeast–southwest strip about 450 km wide, extending from the Luzon Strait to the Vietnam coast. Generally, the mean mesoscale variance in the northern strip tends to be stronger than that in the southern one because more eddies propagate westward along the northern boundary (Wang et al. 2000, 2003).

Using a merged sea surface height anomaly (SSHA) dataset from 1993 to 2000, Wang et al. (2003) find that most of the SCS eddies originated in areas southwest of Taiwan, west of Luzon, Philippines, and east of central Vietnam. Those eddies originated at the eastern SCS,

---

*Corresponding author address:* Dr. Guihua Wang, State Key Laboratory of Satellite Ocean Environment Dynamics, Second Institute of Oceanography, State Oceanic Administration, Hangzhou, China.  
E-mail: guihua\_wanggh@yahoo.com.cn

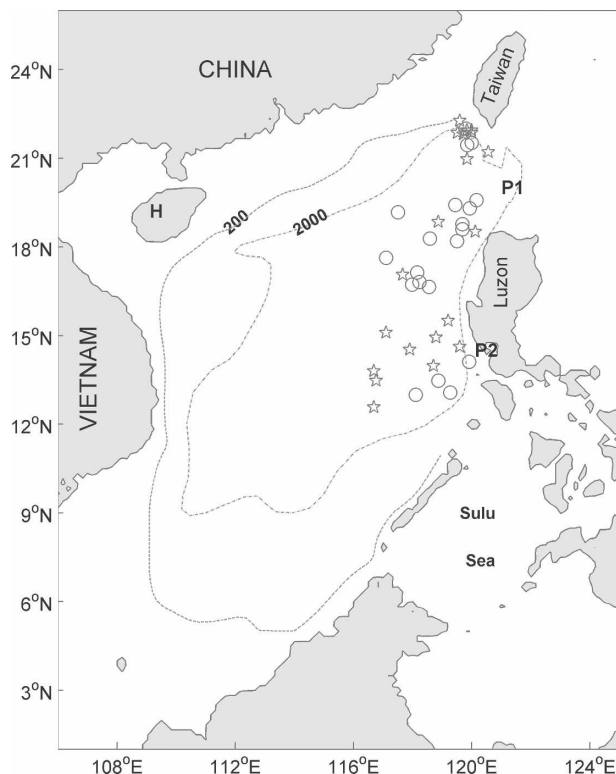


FIG. 1. Map of the SCS (P1: Luzon Strait; P2: Manila Bay; H: Hainan Island). The two isobaths are for 200 and 2000 m. Circles and stars indicate the initial positions of the cyclonic and anticyclonic eddies, respectively, generated in the eastern SCS during the winter periods of January 1993–July 2002.

where the water depths are generally over 2000 m; all migrate in a generally westward direction after they are formed. To the extent possible, Wang et al. (2003) have also used subsurface hydrographic data to support several of their identified eddies from the altimetry data. Wang et al. (2005) further point out that, during the winter monsoon periods, alternating clusters are dominated by anticyclonic eddies in areas southwest of Taiwan and north of Manila Bay, and cyclonic eddies in areas northwest of Luzon and south of Manila Bay (Fig. 1). They also note that these clusters of anticyclonic and cyclonic eddies are correlated, respectively, to the strong negative and positive wind stress curls because of orographic effects.

Several previous studies have associated some of the mesoscale eddies observed in the eastern SCS with wind forcing. For example, Wang and Chern (1987) suggest that an anticyclonic eddy observed southwest of Taiwan in their 1974 hydrographic survey may result from the joint effect of winter monsoon and the Kuroshio. Both Qu (2000) and Metzger (2003) note the existence of a cyclonic eddy offshore of northwest Luzon during the winter and point out its likely connection to

the positive wind stress curl prevailing there. Yang and Liu (2003) suggest that the cyclonic eddy off northwest Luzon behaves like a wind-forced Rossby wave.

The fact that orographic wind jets normal to a coast can generate eddies has long been known [e.g., see the review of Willett et al. (2006) for eddies off the southeast coast of Tehuantepec, Mexico]. Willett et al. (2006) have also reviewed other mechanisms that may contribute to eddy genesis there. The general picture of the eastern SCS as a breeding ground for mesoscale eddies due to orographic winds is still not clear, and the relatively stable spatial distribution of the eddies generated there needs further exploration. In this paper, we will use both satellite data and numerical model experiments to examine the effects of wind stress curl as a generation mechanism for the mesoscale eddies in the eastern SCS during the winter.

## 2. Data and model

The main wind dataset used here comes from the observations by the SeaWinds scatterometer on the Quick Scatterometer (QuikSCAT) space mission of the National Aeronautics and Space Administration (NASA), one of the best-resolved wind products available. To construct a set of wind forcing with various temporal and spatial resolutions, we first averaged the data spatially into  $0.25^\circ$ ,  $0.5^\circ$ ,  $1^\circ$ , and  $2^\circ$  squares and then averaged them in time at intervals of 1, 7, 15, and 30 days, resulting in a total of 16 different time series of wind fields. The standard case of this study has a temporal resolution of 1 day and a spatial resolution of  $0.25^\circ$  latitude  $\times$   $0.25^\circ$  longitude. Another wind product considered here is from the popular reanalysis of the National Centers for Environmental Prediction (NCEP). This dataset has a temporal resolution of 1 day and a spatial resolution of about  $1.875^\circ$  on a Gaussian grid. The NCEP product has been widely applied previously in studies of the SCS (e.g., Shaw et al. 1999; Metzger 2003).

We have also used altimetry SSHA data in this study for both eddy identification and model data comparison. This dataset is constructed by the Space Oceanography Division of the Collecte Localisation Satellites (CLS), based on multiple altimeters from the Ocean Topography Experiment (TOPEX)/Poseidon (T/P), European Remote Sensing Satellite (ERS), and *Environmental Satellite (Envisat)*. It is on a  $1/3^\circ \times 1/3^\circ$  grid and has a temporal resolution of 7 days. The orbit errors have been removed from the SSHA time series with a global multimission crossover minimization method (Le Traon and Ogor 1998). A global tide model is also used to remove tidal signals (Ray 1999). The

SSHA data, as well as the above wind products, cover the period from August 1999 to July 2002. In this paper boreal winter is defined as the period from 1 October to 31 March, because the winter monsoon starts to cover the entire SCS in October, develops fully in January (the wind speed peaks in this month), weakens from January to March, and ends in April.

A 1.5-layer nonlinear reduced-gravity model is used here to simulate the wind-driven upper-ocean dynamics, particularly the eddy generation over the deep water along the eastern SCS by the wind jets from orographic effects. The validity and effectiveness of such a simple model to study eddy generation dynamics over deep water have been demonstrated by many studies (e.g., Reszka and Swaters 1999; Arruda et al. 2004; Zamudio et al. 2006). Its usefulness in simulating eddy generation due to the orographic wind jets from mountain gaps, or isthmus wind jets, has been summarized by Willett et al. (2006). Many previous studies of the SCS upper-layer circulation have also employed such a simple model (e.g., Metzger and Hurlburt 1996; Liu et al. 2001; Wang et al. 2006), including a study of eddy genesis through vorticity advection from the Kuroshio (Liu and Su 1992).

Our model boundary is along the 200-m isobaths (Fig. 1). To focus on the regional dynamics within the SCS, we close the Luzon Strait for most of our experiments. In several specific simulations, however, we include the Kuroshio as a driving force and leave the Luzon Strait open. The reduced gravity is set as  $0.03 \text{ m s}^{-2}$ , the lateral friction coefficient as  $500 \text{ m}^2 \text{ s}^{-1}$ , and the initial thermocline depth as 200 m. The model grids are  $0.25^\circ \times 0.25^\circ$ . The grid size is smaller than the climatological mean first-baroclinic Rossby radius of deformation for the deep basin of the SCS, which is larger than 50 km (Gan and Cai 2001). The model is spun up with the winds switched on gradually from rest to the wind distribution of 1 August 1999 over a 1-month period. The model is then run with the wind data of the whole year from 1 August 1999 to 31 July 2000 repeatedly for four years, until the ocean circulation reaches a quasi-equilibrium state. At last, the model is forced from 1 August 1999 to 31 July 2002 with either the standard QuikSCAT or NCEP winds, and with the QuikSCAT wind subsampled into different resolutions.

### 3. Results

#### *a. Clusters of mesoscale eddies and areas of strong wind stress curl*

Figure 1 depicts the initial positions of the mesoscale eddies generated in the eastern SCS during the winters

of 1993–2002, as identified from the altimeter data. The method used to identify the initial position of an eddy has been described in Wang et al. (2003). The anticyclonic eddies cluster principally in two areas, namely, southwest of Taiwan and west of Manila Bay. The cyclonic eddies also cluster largely in two areas, namely, northwest of Luzon and southwest of Manila Bay. It is obvious that the four clusters are arranged in an alternating order from the north to the south along the eastern boundary of the SCS.

Figure 2a shows the winter-mean QuikSCAT wind vector and wind stress curl fields. A northeast–southwest-oriented zero-curl contour extends approximately from the Taiwan Strait to the offshore region of central Vietnam, separating the SCS into a southeastern region and a northwestern region with positive and negative wind stress curls, respectively. Along the eastern boundary of the SCS, there are two small areas over waters deeper than 200 m with strong negative wind stress curl. South of each is another small area of rather strong positive wind stress curl. Comparing Figs. 1 and 2a, we see that clusters of the anticyclonic and cyclonic eddies correspond to the areas of negative and positive wind stress curls, respectively. Such good correlation indicates that the wind field may play an important role in the generation of these eddies in the eastern SCS during the winter monsoon season.

In Fig. 2a, the island mountain ranges with elevations higher than 500 m are shaded in black. Apparently, the northeast monsoonal winds are blocked and redirected by these high mountains. Narrow, intense wind blow through the gaps of the mountain ranges, forming isthmus wind jets. Two of these jets blowing over the model domain are marked as thick solid blue lines in Fig. 2a. Associated with each of these isthmus wind jet is a dipole of wind stress curl (negative curl to the north of the jet and positive to the south), which collectively form a series of mesoscale wind stress curl cells with alternating signs along the eastern boundary of the SCS.

#### *b. Genesis of mesoscale eddies in the eastern SCS during winter*

Figure 3b displays the winter-mean thermocline depth anomaly from the model experiment driven by the QuikSCAT wind. It is clear that the winter-mean circulation in the eastern SCS is characterized by a series of alternating anticyclonic and cyclonic subbasin gyres, or eddies. Cyclonic eddies are produced west of Luzon Island and south of Manila Bay, and anticyclonic eddies southwest of Taiwan and north of Manila Bay. Such alternating eddies also appear in the mean SSHA field derived from altimetry though their shape and

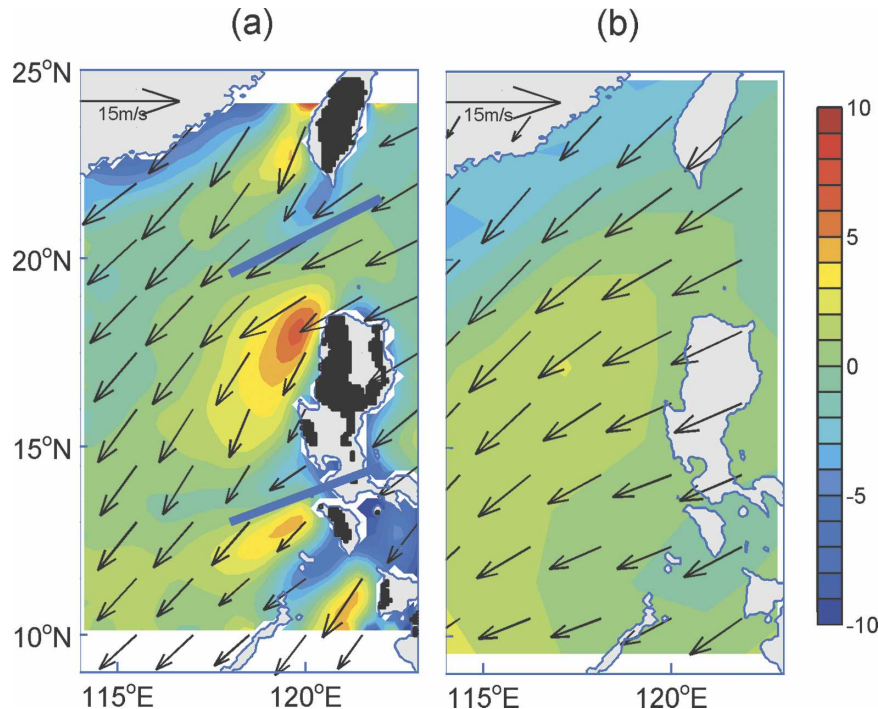


FIG. 2. (a) QuikSCAT and (b) NCEP wind vector ( $\text{m s}^{-1}$ ) and wind stress curl ( $\text{N m}^{-2}$ , color shading) fields averaged for the winters of August 1999–July 2002. In (a), the land topography with elevations greater than 500 m is shaded in black, and the narrow wind jets deeper than 200 m along the eastern boundary of the SCS are indicated as the two thick solid bars.

magnitude are different (Fig. 3a). Not surprisingly, there is a strong correspondence between these (mean) eddies and the observed mean wind stress curls in the eastern SCS (Fig. 2a). Thus the winter eddies in the eastern SCS are likely driven by the wind stress curls associated with the isthmus wind jets through the gaps of the island chain. Spinup of cyclonic and anticyclonic eddies on either side of the axis of an offshore wind jet may be attributed to Ekman pumping (McCreary et al. 1989; Willett et al. 2006). In fact, the summer eddies off central Vietnam are also forced by an orographic wind jet (Xie et al. 2003; Wang et al. 2006). Similar orographically induced features in thermocline depth and currents are also observed elsewhere (e.g., Xie et al. 2001). Once they are generated, these eddies propagate westward because of the beta effect and the westward advection by winter cyclonic basin gyre, as indicated by the elongated eddy features in both the winter-mean observations and numerical results.

The above results indicate that local wind stress curl is likely to be a dominant driving force to spin up the mesoscale eddies in the eastern SCS. However, most of these eddies were not well reproduced in previous models of the SCS. A possible explanation is that the resolution of the wind forcing used for those models was not

high enough for realistic simulation (Metzger 2003). Figure 2b shows the winter-mean wind vector and wind stress curl of the NCEP wind. As compared with the QuikSCAT wind field shown in Fig. 2a, the mesoscale features are now smeared out in the low-resolution NCEP wind product. There is no longer any evidence of alternating cells of wind stress curl along the eastern side of the SCS (Fig. 2b), nor the existence of the isthmus wind jets. Indeed, the modeled winter-mean circulation driven by the NCEP wind (Fig. 3c) no longer has the kind of mesoscale eddy patterns as in Fig. 3b. To further evaluate the effects of wind forcing resolution on eddy generation, we have carried out an additional set of model experiments using 16 different temporal and spatial resolutions of wind fields as described in section 2. The eddy generation is found to be more sensitive to the spatial resolution than the temporal resolution of wind forcing. In particular, when the spatial resolution is larger than  $2^\circ$ , the cyclonic eddy in south Manila Bay will disappear even if the temporal resolution is the highest. In the following, all our discussions on the simulated results will be confined to the model driven by the highest spatial and temporal resolution of the QuikSCAT wind field.

Despite the general agreement, the model simulation

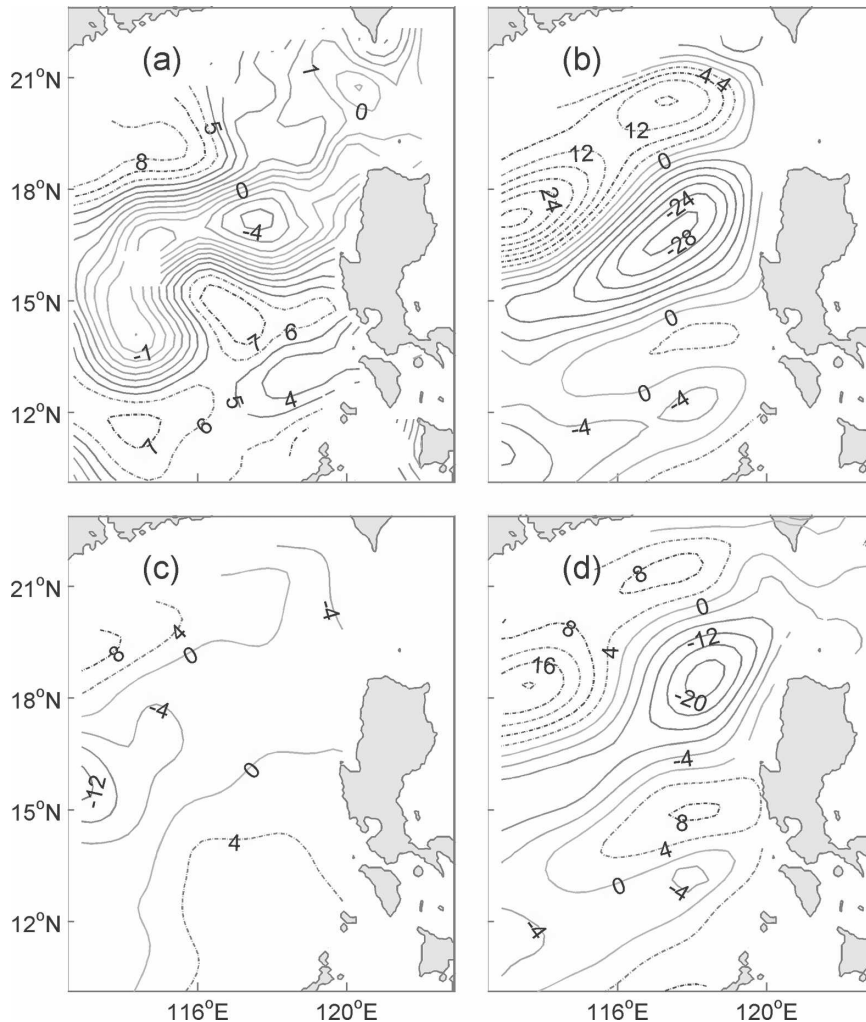


FIG. 3. (a) Observed sea surface height anomaly (cm) from altimetry, and model thermocline depth anomaly (m) driven by (b) QuikSCAT wind, (c) NCEP wind, and (d) both QuikSCAT wind and Kuroshio. All these fields are averages over the winters of August 1999–July 2002.

differs noticeably from observations (Figs. 3a and 3b), especially near the northern boundary of the model domain. In addition, the model-generated eddies and their elongated tracks are shifted somewhat southward as compared to those observed. A possible cause of this disagreement is the close-up of the Luzon Strait in the standard experiment, which prevents the influence of the Kuroshio from entering the SCS. To examine the potential impact of the Kuroshio, we opened the Luzon Strait and specified a Kuroshio input along the zonal section  $18^{\circ}\text{N}$ ,  $122^{\circ}$ – $124.5^{\circ}\text{E}$ . The open boundary conditions are set as done by Hurlburt and Thompson (1980). The result of this experiment (Fig. 3d) does not show much improvement except near the northern boundary, where the unrealistically strong variability in the case without the Kuroshio (Fig. 3b) is much re-

duced. There is no doubt that our simple model cannot simulate well the intrusion dynamics of the Kuroshio across the Luzon Strait. The fact that we define the 200-m isobaths as a solid wall also makes it difficult to realistically simulate the circulation near the boundaries.

The modeled winter-mean thermocline depth anomaly (Fig. 3b) is the average for the three winters during 1 August 1999 to 31 July 2002. Our numerical model is generally successful in simulating the genesis, propagation, and dissipation of individual eddies. Table 1 illustrates the extent that the wind-driven forcing mechanism can explain the generation of individual eddies observed in the eastern SCS. Out of the 13 eddies observed from the altimetry data during the winters of this period, 9 eddies are reproduced by our simple nu-

TABLE 1. Comparison of eddy characteristics between the model simulation (MOD) [some were not simulated (NS)] without the presence of the Kuroshio and the observation (OBS) from altimetry data. The eddies are listed according to the latitudes of their initial observed position. Initial appearance: dates of initial identification of the eddy in the format year, month, and day (yyyymmdd). Type: anticyclonic (A) and cyclonic (C). [Methodology used to identify the initial appearance and termination of an eddy is given in Wang et al. (2003). The same criteria are applied for the characteristics of both the simulated and the observed eddies.]

Type	Initial position ( $^{\circ}$ N, $^{\circ}$ E)		Initial appearance		Life span (day)		Distance traveled (km)	
	OBS	MOD	OBS	MOD	OBS	MOD	OBS	MOD
A	22.27, 119.60	21.30, 119.00	19991015	19991005	140	70	240	370
A	22.24, 119.95	21.02, 119.04	20001115	20001025	150	140	210	350
C	22.00, 119.80	NS	20020225					
A	21.81, 119.72	21.11, 119.22	20001205	20001120	50	70	350	450
C	21.52, 120.00	NS	20011005					
A	18.51, 120.12	NS	20020305					
C	18.25, 118.90	17.00, 118.85	20000115	20001205	160	170	430	567
C	18.20, 119.50	16.80, 119.00	20011025	20011015	90	110	510	700
C	18.17, 118.70	16.95, 118.80	19991225	19991215	200	220	460	595
C	16.65, 118.55	NS	19991205					
C	15.50, 119.20	14.10, 119.02	20011105	20011025	70	80	820	900
A	15.10, 117.10	14.30, 119.05	20000125	20000115	150	110	630	535
A	14.62, 119.60	13.82, 119.12	20011205	20011125	50	70	480	570

merical model. The initial positions of these nine simulated eddies are somewhat south of the observed ones. This may be partly a result of replacing the 200-m isobaths by a solid wall in our model. The remaining four eddies not reproduced by our model may be generated by other mechanisms, such as barotropic or baroclinic instability. Overall, for winter eddy genesis in the eastern SCS, the proposed wind-driving mechanism seems to be at work.

#### 4. Summary and discussion

The mesoscale eddy activity is particularly rich in the SCS (Su et al. 1999), and the eastern part of the basin has been previously identified as a breeding ground of eddies during winter months (Wang et al. 2003). To our best knowledge, the study presented here is the first to consider the wind jets through island gaps as a driving mechanism for eddy genesis in the SCS. We have used both observational evidence and model experiments to show that the wind stress curls associated with these jets can spin up cyclonic and anticyclonic eddies on the two sides of each jet. Collectively, this explains the observed alternating anticyclonic and cyclonic eddy pattern in the eastern SCS from both hydrographic surveys and altimeter observations.

The SCS circulation is largely driven by the east Asian monsoon, and the winter gap winds along the eastern boundary of the SCS are intrinsic regional features of the monsoon due to orographic effects. Thus a realistic dynamical simulation of this important marginal sea depends crucially on accurate observations of

surface wind forcing. As compared with the NCEP reanalysis wind, the high-resolution QuikSCAT product improves model simulations of the SCS, especially in terms of the mesoscale features found in winter. The improvement is attributed to the better-resolved wind stress curl fields associated with the gap winds. The deficiency of the reanalysis wind is likely to be a result of unresolved orography.

As long as the gap winds are well resolved, eddy generation in the model is not particularly sensitive to the resolution of wind forcing, nor is it dependent on the inclusion of the Kuroshio, although the latter makes the simulation more realistic in the far north SCS. Nevertheless, there still remain some discrepancies between simulated and observed eddies in the eastern SCS, possibly because of the deficiencies of our model. Although the simple reduced-gravity model captures the essential wind-driven ocean dynamics and thus is able to grossly simulate the eddy generation process at work here, a more faithful simulation of the mesoscale activities in the SCS will require a general circulation model with complete physics.

*Acknowledgments.* This study was supported by National Basic Research Program of China (2007CB816003), NSFC Grants (40676007 and 40520140073), "863" Hi-tech Program (2006AA09Z156), and by NASA OSTST and OVWST programs.

#### REFERENCES

- Arruda, W., D. Nof, and J. J. O'Brien, 2004: Does the Ulleung eddy owe its existence to beta and nonlinearities? *Deep-Sea Res. I*, **51**, 2073–2090.

- Chu, P. C., C. W. Fan, C. J. Lozano, and J. L. Kerling, 1998: An airborne expendable bathythermograph survey of the South China Sea, May 1995. *J. Geophys. Res.*, **103**, 21 637–21 652.
- Gan, Z. J., and S. Q. Cai, 2001: Geographical and seasonal variability of Rossby Raddi in South China Sea. *J. Trop. Oceanogr.*, **20**, 1–9.
- Hurlburt, H. E., and J. D. Thompson, 1980: Numerical study of Loop Current intrusions and eddy shedding. *J. Phys. Oceanogr.*, **10**, 1611–1651.
- Hwang, C., and S. A. Chen, 2000: Circulations and eddies over the South China Sea derived from TOPEX/Poseidon altimetry. *J. Geophys. Res.*, **105**, 23 943–23 965.
- Le Traon, P.-Y., and F. Ogor, 1998: ERS-1/2 orbit improvement using TOPEX/POSEIDON: The 2 cm challenge. *J. Geophys. Res.*, **103**, 8045–8057.
- Liu, X. B., and J. L. Su, 1992: A reduced gravity model of the circulation in the South China Sea (in Chinese). *Oceanol. Limnol. Sin.*, **23**, 167–174.
- Liu, Z. Y., H. J. Yang, and Q. Y. Liu, 2001: Regional dynamics of seasonal variability in the South China Sea. *J. Phys. Oceanogr.*, **31**, 272–284.
- McCreary, J. P., H. S. Lee, and D. B. Enfield, 1989: The response of the coastal ocean to strong offshore winds: With application to circulations in the Gulfs of Tehuantepec and Papagayo. *J. Mar. Res.*, **47**, 81–109.
- Metzger, E. J., 2003: Upper ocean sensitivity to wind forcing in the South China Sea. *J. Oceanogr.*, **59**, 783–798.
- , and H. Hurlburt, 1996: Coupled dynamics of the South China Sea, Sulu Sea, and the Pacific Ocean. *J. Geophys. Res.*, **101**, 12 331–12 352.
- , and H. Hurlburt, 2001: The nondeterministic nature of Kuroshio penetration and eddy shedding in the South China Sea. *J. Phys. Oceanogr.*, **31**, 1712–1732.
- Qu, T. D., 2000: Upper-layer circulation in the South China Sea. *J. Phys. Oceanogr.*, **30**, 1450–1460.
- Ray, R., 1999: A Global Ocean Tide model from TOPEX/Poseidon altimetry, GOT99.2. NASA Tech. Memo. NASA/TM-1999-209478, Goddard Space Flight Center, Greenbelt, MD, 58 pp.
- Reszka, M. K., and G. E. Swaters, 1999: Eddy formation and interaction in a baroclinic frontal geostrophic model. *J. Phys. Oceanogr.*, **29**, 3025–3042.
- Shaw, P. T., S. Y. Chao, and L. L. Fu, 1999: Sea surface height variation in the South China Sea from satellite altimetry. *Oceanol. Acta*, **22**, 1–17.
- Su, J. L., 2004: Overview of the South China Sea circulation and its influence on the coastal physical oceanography near the Pearl River estuary. *Cont. Shelf. Res.*, **24**, 1745–1760.
- , J. P. Xu, S. Q. Cai, and O. Wang, 1999: Gyres and eddies in the South China Sea. *Onset and Evolution of the South China Sea Monsoon and Its Interaction with the Ocean* (in Chinese), PP423, Y. Ding and C. Li, Eds., China Meteorological Press, 272–279.
- Wang, G., J. Su, and P. C. Chu, 2003: Mesoscale eddies in the South China Sea detected from altimeter data. *Geophys. Res. Lett.*, **30**, 2121, doi:10.1029/2003GL018532.
- , —, and R. F. Li, 2005: Mesoscale eddies in the South China Sea and their impact on temperature profiles. *Acta Oceanol. Sin.*, **24**, 39–45.
- , D. Chen, and J. Su, 2006: Generation and life cycle of the dipole in South China Sea summer circulation. *J. Geophys. Res.*, **111**, C06002, doi:10.1029/2005JC003314.
- Wang, J., and C. S. Chern, 1987: The warm-core eddy in the northern South China Sea (in Chinese). *Acta Oceanogr. Taiwanica*, **18**, 92–112.
- Wang, L. P., C. J. Koblinsky, and S. Howden, 2000: Mesoscale variability in the South China Sea from the TOPEX/Poseidon altimetry data. *Deep-Sea Res. I*, **47**, 681–708.
- Willett, C. S., R. R. Leben, and M. F. L. Peregrina, 2006: Eddies and tropical instability waves in the eastern tropical Pacific: A review. *Prog. Oceanogr.*, **69**, 218–238.
- Xie, S.-P., W. T. Liu, Q. Liu, and M. Nonaka, 2001: Far-reaching effects of the Hawaiian Islands on the Pacific Ocean-atmosphere system. *Science*, **292**, 2057–2060.
- , Q. Xie, D. X. Wang, and W. T. Liu, 2003: Summer upwelling in the South China Sea and its role in regional climate variations. *J. Geophys. Res.*, **108**, 3261, doi:10.1029/2003JC001876.
- Yang, H., and Q. Y. Liu, 2003: Forced Rossby wave in the northern South China Sea. *Deep Sea Res. I*, **50**, 917–926.
- Zamudio, L., H. E. Hurlburt, E. J. Metzger, S. L. Morey, J. J. O'Brien, C. Tilburg, and J. Zavala-Hidalgo, 2006: Interannual variability of Tehuantepec eddies. *J. Geophys. Res.*, **111**, C05001, doi:10.1029/2005JC003182.